REVIEW ARTICLE

THE ELECTROOXIDATION OF CO: A TEST REACTION IN ELECTROCATALYSIS

B. Beden and C. Lamy

Laboratoire de Chimie I, Electrochimie et Interactions, UA CNRSn° 350, Université de Poitiers,
40 Avenue du recteur Pineau, 86022 Poitiers, France

N. R. de Tacconi and A. J. Arvia

Instituto de Investigaciones Fisicoquímicas Teóricas y Aplicadas (INIFTA), Facultad de Ciencias
Exactas, Universidad Nacional de La Plata, C.C. 16, Sucursal 4, 1900 La Plata, Argentina

Abstract—This review paper aims to show how the electrochemical behaviour of CO plays a key role in the understanding of the reaction mechanism of many electrocatalytic oxidations of small organic molecules. For that purpose, the adsorption of CO on noble metal electrodes, eventually modified by foreign metal adatoms, is reviewed, taking into account both experimental (electrochemical and spectroscopic techniques) and theoretical (Extended Hückel Model) approaches. Data from the gas phase–solid metal interface are also considered.

1. INTRODUCTION

The voltammetric electrooxidation of carbon monoxide on polycrystalline (pc) platinum or pc rhodium, either in acid or alkaline solutions, exhibits multiple current peaks in a rather narrow potential domain. This fact points out the complex nature of the corresponding electrochemical reaction[1–4]. To understand the origin of these current peaks is of outmost importance because it has been shown[5] that carbon monoxide is formed during the course of many electrocatalytic reactions involving small size organic molecules such as methanol, formic acid, . . .

Earlier cyclic voltammetry experiments have been extended in two ways by using combined perturbing potential programs which led to the quantitative evaluation of the adsorbed species at the electrode surface[6, 7], and by applying new reflection spectroscopy techniques, particularly in the infrared region, which allowed *in situ* identification of the adsorbed species by their vibrational spectra[8, 9].

The results obtained throughout the application of those techniques have clearly shown not only the sensitivity of the electrooxidation of CO to usual parameters such as pH, temperature and solution composition, but also the strong dependence of the reaction on the electrode surface state, that is in terms of morphology and structure. Experiments have been

run so far on different types of platinum electrodes, namely, smooth and rough pc Pt, Pt(100), Pt(110) and Pt(111) single crystals and Pt with preferred crystalline orientations (pco) prepared through suitable pulsing methods developed at INIFTA[10].

In recent years the cooperative work made on the electrooxidation of CO and small organic fuels on noble metal electrodes, at INIFTA, University of La Plata, Argentina (electrochemical techniques) and at the Electrochemistry Laboratory, University of Poitiers, France (spectroscopic techniques) has contributed with new original information. The present article is a review of the recent achievements on the matter in which the contributions of our cooperative work are summarized. Most of the work refer to very recently reported data. For a general view on the subject the reader is referred to the literature[1, 2, 11, 12] which contains an extended review of previous studies.

A chronological presentation of the results related to the electrosorption of CO on different metals of electrocatalytic interest has been made in order to account for the evolution of concepts, development and improvement of in situ reflexion spectroscopy techniques. Then, the participation of CO as a poison in many electrocatalytic reactions and the influence of the metal surface characteristics are discussed on the basis of new data obtained by Electromodulated Infrared Reflectance Spectroscopy (EMIRS). Finally, attention is focused on the perturbation of the *ir* spectrum of a CO monolayer on Rh in the presence of some foreign adatoms. These results allow us to measure the number of adsorption sites that they occupy, and to advance in the comprehension of electrocatalytic reactions.

This work is dedicated to the memory of Professor Maria Cristina Giordano.

A list of review articles published since January 1986 is given on p. 793 of this issue.
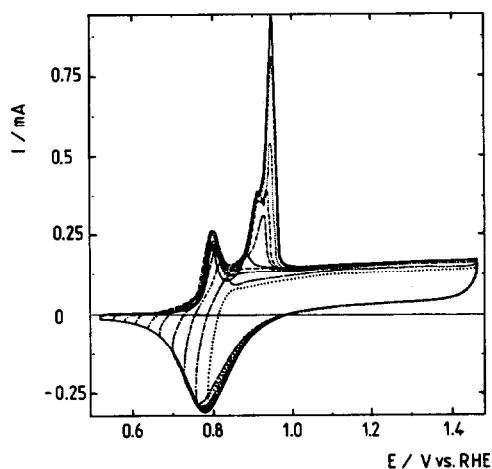
Fig. 1. Voltammograms of a polycrystalline Pt electrode in a 1 M HClO$_4$ solution saturated with gaseous CO, at different lower potential limits, E_c ($v = 100$ mV s^{-1}; 25°C): (°°°) = 0.80; (-°-°-) = 0.77; (-xx-xx-) = 0.74; (—·—·) = 0.71; (-x-x-) = 0.68; (-·····-) = 0.65; (-····-) = 0.62; (. . .) = 0.59; (- - -) = 0.56; (———) = 0.53 V.

Fig. 2. Adsorption of CO on a pc. Pt electrode immersed in a 1 M HClO$_4$ solution saturated with gaseous CO. The degree of surface coverage, Θ, by the two adsorbed species, CO$_L$ and CO$_B$, is given as a function of t_{ad}. $E_{ad} = 0.59$ V/rhe, 25°C: (●) Θ_H; (□) Θ_{CO}^B; (○) Θ_{CO}^L; (△) $\Theta_{CO}^T = \Theta_{CO}^B + \Theta_{CO}^L$.

2. ADSORPTION OF CO ON NOBLE METAL ELECTRODES

2.1. Polycrystalline platinum

The current (I)–potential (E) curves (Fig. 1) obtained at a sweep rate $v = 0.1$ V s^{-1} for a smooth pc Pt immersed in 1 M HClO$_4$, by keeping the upper potential limit constant, $E_a = 1.45$ V (rhe) and gradually decreasing the lower potential limit, E_c, show several electrooxidation current peaks. The appearance of these peaks is related, in a first approximation, to the time the electrode was in contact with the CO-containing solution after the electroreduction of the O-adatom layer[3, 7]. Similar results but with an even higher peak multiplicity have been obtained in basic solutions[4, 13].

By setting the adsorption time (t_{ad}) and the adsorption potential (E_{ad}) by means of voltammetric runs with combined potential programs (VCPP), it is possible to achieve the quantitative separation of at least two CO species[7, 14]. The interpretation of these results shows that for small values of t_{ad} ($t_{ad} < 4$ s) the adsorption of each CO$_{ad}$ species involves 2 (or more) adsorption sites, whereas the remaining sites are occupied by H-adatoms. Otherwise, large values of t_{ad} ($t_{ad} > 12$ s), lead to the maximum coverage of the substrate by linearly adsorbed CO species (Fig. 2). The latter has been unambiguously identified throughout the evaluation of the number of electrons per site, N_{eps}, which are necessary to carry on the electrooxidation of CO$_{ad}$, as far as linearly adsorbed CO is the* only species involving the value $N_{eps} = 2$.

2.2. Platinum single crystals

The sensitivity of CO adsorption to the crystalline structure of the substrate has been investigated, by potential programme voltammetry (PPV), on low Miller indices single crystal platinum surfaces, namely
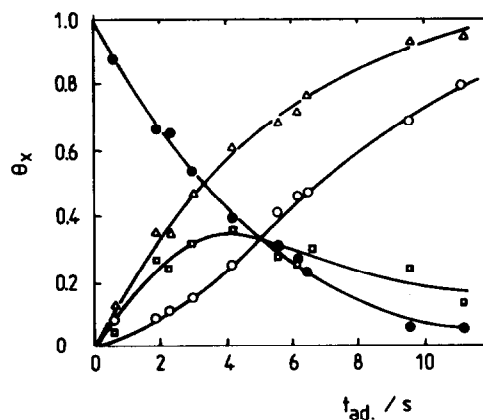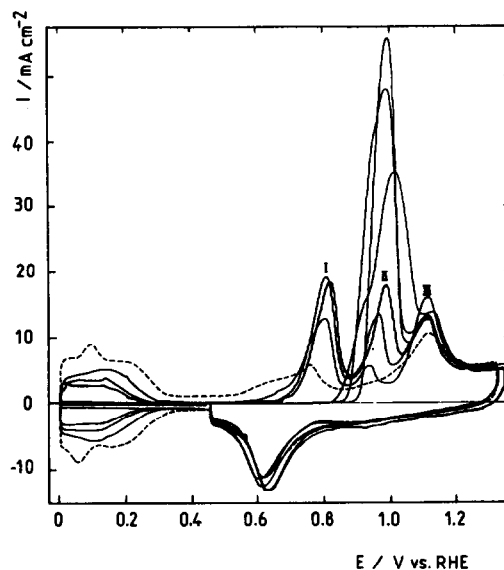

Fig. 3. Voltammograms of a Pt(111) single crystal electrode in 0.5 M HClO$_4$ saturated with gaseous CO for different adsorption times ($1.2 < t_{ads} < 25$ s). $E_{ads} = 0.45$ V/rhe; 25°C; $v = 10$ V s^{-1}; (---) = supporting electrolyte.

Pt(100), Pt(110) and Pt(111). The electrode surfaces were prepared by thermal treatment and characterized through the H-atom electroadsorption/electrodesorption voltammograms[15]. In acid medium and for small values of t_{ad}, at least two types of adsorbates have been quantitatively determined on each single crystal plane[16, 17]—see eg Fig. 3 for Pt(111). The substrate saturation coverage by linearly bound CO is obtained in less than 8 s at room temperature for Pt(100) and Pt(110), whereas about 14 s are required for Pt(111). Likewise, the proportion of CO$_{ad}$ species occupying more than one adsorption site is definitely greater for Pt(111) as compared to Pt(100) and

Pt(110). Finally, the potential of the main CO_{ad} electrooxidation peak, under adsorbate saturation conditions, differs appreciably for each plane. For example, for a voltammogram run at 10 V s^{-1}, the main peak appears at 0.95 V, 0.99 V and 1.06 V/rhe respectively for Pt(110), Pt(111) and Pt(100), (17). Very similar results were obtained in alkaline medium[4].

2.3. Preferred oriented platinum

The electrooxidation of CO adsorbates has also been studied at platinum electrodes, on the surface of which type (111) (type I electrode) and type (100) (type II electrode) preferred crystalline orientations (pco) were produced[18]. The electrochemical reaction was followed by voltammetry in acid (0.05 M $HClO_4$) and basic (1 M KOH) solutions[10, 18]. In both cases CO adsorption proceeded from a CO saturated solution for $t_{ad} = 1$ min at $E_{ad} = 0.25$ V/rhe, and the voltammograms were recorded at $v = 0.1 \text{ V s}^{-1}$ by means of the microflux cell technique in order to avoid any interference due to readsorption of CO from solution in the course of the voltammetric run.

For the two types of pco Pt electrodes, the CO_{ad} electrooxidation reaction is characterized by very sharp voltammetric peaks, which correspond as a first approximation to the two main peaks observed for pc Pt under comparable experimental conditions (Fig. 4). The separation of the peak potentials is about 50 mV, a value which agrees well with the difference in the location of the peaks resulting from CO adsorption on Pt(111) and Pt(100) single crystals under saturation adsorption conditions[17]. These results confirm that the pco Pt electrodes behave very similarly to Pt single crystal surfaces. Furthermore, this fact suggests that the multiplicity of voltammetric peaks resulting from

the electrooxidation of adsorbed CO on pc Pt is due to the random distribution of polyoriented crystalline facets on its surface.

2.4. In situ uv–vis reflection spectroscopy (UVERS)

The uv–vis reflectance spectra of smooth pc Pt surfaces immersed in the electrolytic solution containing dissolved CO was followed in situ. It was found that the relative reflectivity of the surface, $(\Delta R/R)$, changes during the progressive coverage by adsorbed CO[19, 20]. The measurements were made at a wavelength value (360 nm), for which there is no light absorption by CO dissolved in solution. The $\Delta R_{CO}/\Delta R_{max}$ ratio vs Θ_{CO} plots provide interesting information about the type of electroadsorbates. ΔR_{CO} is the reflectance change related to the adsorption of CO, and ΔR_{max} the maximum reflectance change referred to the formation of a monolayer of O-containing surface species on platinum. Θ_{CO}, ie the total degree of surface coverage by CO electroadsorbates, is calculated from the voltammetric data, taking into account the decrease in the H-atom voltammetric charge as the CO adsorption is occurring.

The $\Delta R_{CO}/\Delta R_{max}$ ratio vs Θ_{CO} plots show a discontinuity which has been interpreted in terms of the existence of two kinds of CO adsorbates. Despite the fact that the accuracy of the experimental results is not completely satisfactory, it was possible to conclude that the formation of linearly bound CO adsorbate, CO_L, is favoured at high degree of surface coverages and high positive potentials. Conversely, at low degree of surface coverage and low potentials, it appears that at the early stages of surface coverage each CO species occupies more than one adsorption site. This type of species is denoted as CO_B, for bridge-bonded CO and CO_m for multi-bonded CO.

2.5. Electrochemically modulated ir reflectance spectroscopy (EMIRS)

The EMIRS technique, which was brought up to an useful and reliable technique by Bewick et al.[21, 22], particularly to investigate adsorbed species at the electrode–solution interface, has been now extensivey described in specialized books[8, 9].

EMIRS has been applied to study the adsorption of CO on several metals of interest in electrocatalysis. Preliminary results, made in CO saturated solutions, showed, from the very beginning, considerable differences among the various adsorption states of CO[23, 24]. More recently, through the improvement of the EMIRS technique on one hand, and the comparison of these results to the infrared absorption bands obtained at the solid–gas interface on the other hand[25], it was possible to characterize the CO_L species in the 2020–2090 cm^{-1} range, the CO_B species in the 1900–1960 cm^{-1} range and the CO_m species in the 1750–1880 cm^{-1} range. It is also interesting to observe that, under comparable experimental conditions (Fig. 5), the degree of surface coverage of Pt by CO_L reaches a maximum value, whereas the surface coverage degree by CO_{ad} species on Rh involves important contributions of both CO_B and CO_L[23, 26], a situation also found when CO_{ad} is produced by decomposition of formic acid[27]. On the other hand,
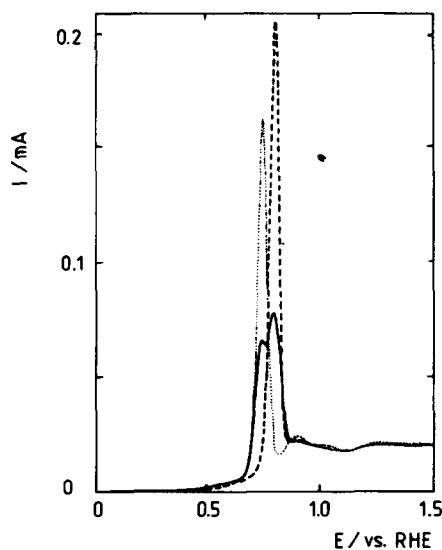
Fig. 4. Voltammograms of adsorbed CO electrooxidation on polycrystalline(——), type I (. . .) and type II (– – –) platinum electrodes. Adsorption potential $E_{ad} = 0.25$ V/rhe; adsorption time $t_{ad} = 1$ min., sweep rate, $v = 0.1 \text{ V s}^{-1}$; 0.05 M $HClO_4$; 25°C. For the preparation of type I and type II electrodes[18].
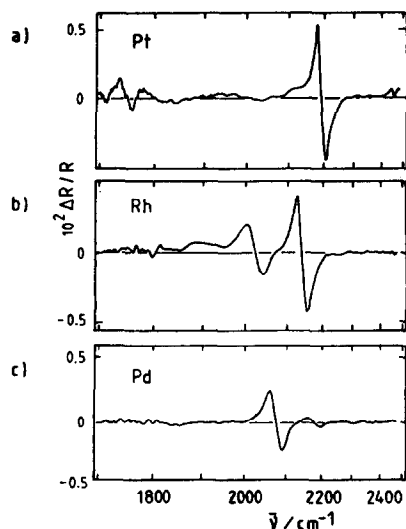
Fig. 5. EMIRS spectra of CO species adsorbed on noble metal electrodes immersed in a 0.5 M HClO₄ solution saturated with gaseous CO. $\Delta E = 400$ mV, $\bar{E} = 0.2$ V vs rhe, f $= 13.5$ Hz: (a) Pt; (b) Rh; (c) Pd.

on palladium, a maximum coverage by CO_B and a minium coverage by CO_L are observed[8, 28, 29]. This behaviour is maintained even for very prolonged adsorption times, in agreement with electrochemical results which show that the limiting value of N_{eps} is already reached as regard to the time scale of the spectroscopic experiment. EMIRS spectra for CO_{ad} species on Pt formed from $^{12}CO + ^{13}CO$ mixtures were also studied[30]. At high coverage, a single bipolar EMIRS band is seen, whose shift in wavenumbers with the $^{12}CO/^{13}CO$ ratio is indicative of a highly coupled system.

A very reproducible appearance of supplementary peaks at around 1640 and 1700 cm⁻¹ can be noticed, particularly for platinum at the initiation of spectral accumulation. They were respectively explained by the presence of adsorbed water, the deformation vibration of which, $\delta(H-O-H)$, absorbing near 1620–1640 cm⁻¹[31], and by the existence of other adsorbed species containing a carbonyl group. It has to be kept in mind that asymmetric OCO stretches of adsorbed formate groups could also contribute strongly to the band at 1640 cm⁻¹.

Attention was focused on the absorption band of CO at the platinum surface by means of new developed spectroscopic techniques, with modulation of the polarization state of the incident light beam[32], by Fourier transform infrared spectroscopy (FT-ir)[33, 34], or by coupling the two spectroscopic techniques[35]. After these extensive studies[35-37], it is now understood that the frequency shift of the absorption band center as a function of the applied potential, of ca 30 cm⁻¹ V⁻¹, is due to a pure Stark effect[38, 39]. This explains the bipolar shape of the EMIRS bands which emerge from the fact that the modulating effect of the electrode potential acts only on the force constant of the CO bond. Then, the modulated optical response is directly proportional to the adsorbate surface coverage degree.

3. RELEVANCE OF CO_{ad} IN ELECTROCATALYTIC POISONING

3.1. CO_{ad} as a poison in the course of electrocatalytic reactions

The formation of CO_{ad} on platinum electrodes has been early observed through EMIRS as resulting from the decomposition of methanol[40] or formic acid[41] in acid solutions. However, a number of years had to pass before the idea became accepted in electrocatalysis[42]. This delay was due in part to the poor knowledge about the exact role of CO, ie either it was a reactive intermediate or only a poison, and also in part because it was difficult to introduce CO_{ad} into the reaction scheme proposed by Bagotskii et al. in the 1970s[43] following the initial idea of Sokolova[44]. The first quantitative studies of Kunimatsu et al. [35-37, 45] seemed to confirm the presence of CO_{ad}, however at variance with the data from combined mass spectroscopy and voltammetry which appeared to be in favour of a COH or CHO intermediate[46, 47]. The main objection to the EMIRS data was that the existence of a single adsorbate, CO_{ad}, was insufficient to explain the different voltammograms obtained on platinum with CO, CH_3OH or HCOOH as electroactive species. It should be mentioned that recent investigations with other molecules such as ethylene glycol[48, 49], ethanol[50-52] and other systems, such as formaldehyde on palladium, platinum and rhodium electrodes[53], and formic acid on rhodium[27, 54], further confirm always the presence of CO as a product of these electrocatalytic reactions[9, 42], except when platinized glassy carbon electrodes are used[55].

The ideas which then came out were that the adsorption time played a major role and that the experimental conditions selected for EMIRS, involving long spectral accumulation times used to increase the signal-to-noise ratio and relatively high concentrations in the electroactive species, favoured the satura-
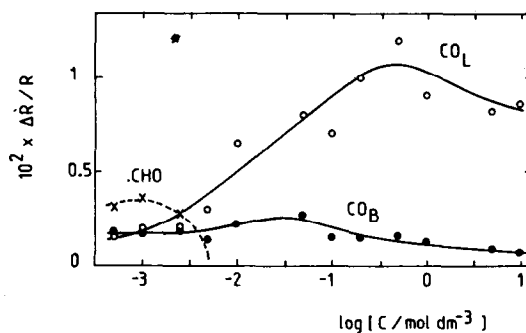

Fig. 6. Peak to peak intensity of the ir signals due to the three EMIRS bands observed in the wavenumber range 1600–2200 cm⁻¹ when methanol is chemisorbed at a pc Pt electrode, as a function of methanol concentration. ΔE $= 400$ mV, $\bar{E} = 0.2$ V/rhe, $f = 13.6$ Hz, 25°C, 30 averaged scans. The CH_3OH concentration is varied from 10^{-3} to 10 M, in a 0.5 M HClO₄ solution. The bands detected are located at ca 2060 cm⁻¹ (linearly bonded CO_L), ca 1870 cm⁻¹ (bridge-bonded CO_B) and ca 1690 cm⁻¹ (.CHO-type species), depending on methanol concentration.

tion of the substrate with CO_{ad}, so that other weakly-bound adsorbates could no longer exist.

Accordingly, to overcome these difficulties new attempts were made following two ways. In one way the concentration of the active species was considerably decreased[56], so that the formation of CO adsorbates in the course of the spectroscopic experiment was drastically delayed (see Fig. 6). The other way, followed by other groups, consisted in the use of a flux cell, so that during the experiment it was possible to renew periodically the electrode surface by applying a positive potential step for oxidizing the adsorbed residues[57, 58]. The results from both types of experiments were in good agreement, at least for the adsorption of methanol on platinum. CO_{ad} is formed rather slowly and replaces irreversibly the species which are less strongly adsorbed[59]. Therefore, CO_{ad} plays the actual role of a catalytic poison.

The change of the corresponding CO absorption bands during the spectral accumulation time is shown in Fig. 7, for a 0.4 V modulation potential centered at 0.2 V/rhe. The increasing contribution of the band centered at ca 2050 cm^{-1}, assigned to CO_L, correlates well with the decreasing amplitude of the complex band lying in the 1630–1730 cm^{-1} range and with the inversion of the peak due to CO_2 at ca 2330 cm^{-1}. The initial band shape and the sign of the latter peak presumably correspond to an adsorption at the lower switching potential where one can predict that no electrooxidation of the electroadsorbate to CO_2 should occur. Nevertheless, the appearance of the CO_2 band is reproducible and is also observed for Methanol[50] or for CO_2 saturated solutions[60]. There is almost no doubts that it corresponds to weakly

adsorbed carbon dioxide. The complex band arises from at least two contributions, the first one at about 1620–1640 cm^{-1}, which is partly due to adsorbed water, the second one, which is more intense, in the 1680–1700 cm^{-1} range. The latter has to be attributed to a carbonyl containing functional group, such as the formyl group –CHO[47, 50, 51, 56, 61]. It is worth mentioning that a very similar band has been reported for either acetaldehyde or acetic acid adsorption on platinum in perchloric acid solutions[50, 61].

3.2. The sensitivity of adsorbed CO to the substrate structure

The distribution of the different CO_{ad} species on the substrate depends strongly on the proper crystalline characteristics of the substrate[62–66]. The EMIRS spectra of the electroadsorbates produced from methanol chemisorption on three different platinum single crystal faces, namely Pt(100), Pt(110) and Pt(111), are illustrated in Fig. 8. As a whole, one can observe through these spectra the same species previously described, but with differences essentially related to the crystalline orientation of the substrate[62, 63]. Thus, the large contribution of the species responsible for the band at 1680–1700 cm^{-1} can only be seen for Pt(100). Furthermore, the band at 1870 cm^{-1}, assigned to CO_B species, becomes considerably intense and single-sided with a positive sign, indicating that the corresponding electroadsorbate has been produced at the lower potential limit. Otherwise, the asymmetry of the EMIRS band, centered at 2050 cm^{-1}, points out a
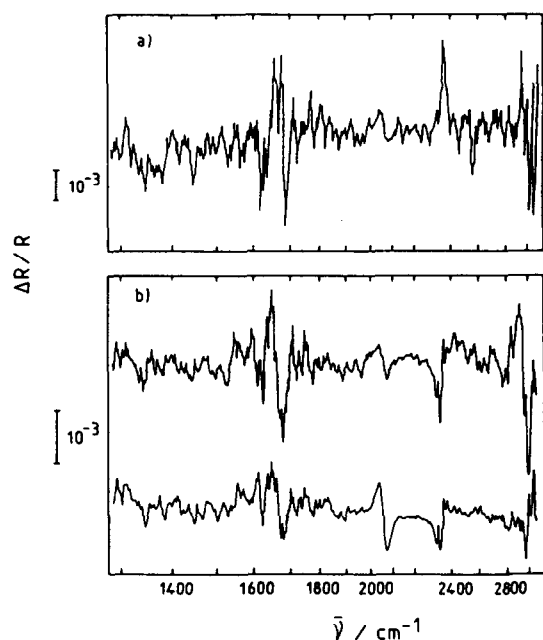

Fig. 7. EMIRS spectra of the species resulting from methanol adsorption on pc Pt as a function of the number of scans, ie of the adsorption time; 0.5 M $HClO_4 + 5 \times 10^{-3}$ M CH_3OH, $\Delta E = 0.4$ V, $\bar{E} = 0.2$ V/rhe, $f = 13.5$ Hz, room temperature: (a) first scan; (b) 10th and 25th scans.
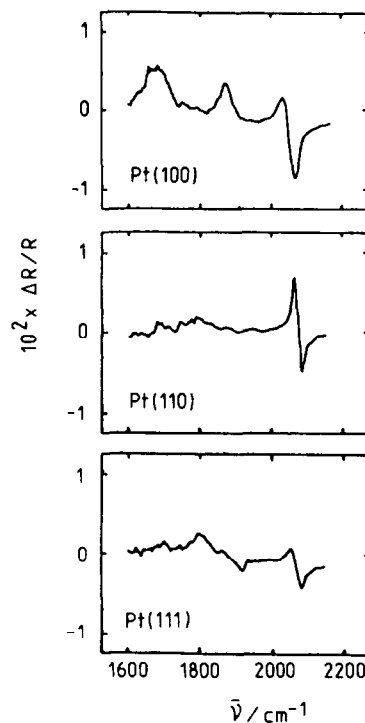
Fig. 8. EMIRS spectra of the adsorbed CO species resulting from the chemisorption of 0.1 M CH_3OH in 0.5 M $HClO_4$ at a Pt single crystal electrode; $\Delta E = 400$ mV, $\bar{E} = 350$ mV/rhe, $f = 13.6$ Hz, exposed face: (a) Pt(100); (b) Pt(110); (c) Pt(111).

higher contribution of CO_L at the upper potential limit.

For Pt(110), the most intense band is that assigned to the CO_L species. It appears centered at 2077 cm^{-1}, that is shifted positively, as it is expected for a higher electroadsorbate surface concentration, in agreement with results obtained for pc Pt. The broad band, covering the 1700–1900 cm^{-1} range, has been assigned to the presence of multibonded CO_m species.

Finally, for Pt(111) one can distinguish a relatively weak absorption band related to CO_L and another one associated with CO_B, the latter presumably involving two contributions. It is interesting to note that the same type of fine structured band has recently been observed at the Pt(111)–CO gas interface[67].

Anions effects were also observed. For instance, if one compares the CO_{ad} EMIRS bands for Pt(hkl) in perchloric acid[62, 63], to those for Pt(hkl) in sulphuric acid[64], it is striking that the CO_B bands are lowered by several tens of wavenumbers in the latter case, while the CO_L bands are nearly not affected. Similarly the CO_L bands were found very recently to be dependent on the reconstruction of the crystalline surface[68]. The "disordered" Pt(111) surface, for instance, leads to a CO_L band upshifted by ca 10 cm^{-1} comparatively to the well ordered Pt(111) crystal.

On an other hand, the detailed inspection and analysis of the EMIRS spectra of CO adsorbates on different Pt surfaces provide new insights to understand some characteristics of the voltammetric response for the electrooxidation of methanol on different crystalline faces of platinum (Fig. 9). Thus, the active site blockage preceding the steep current increase at about 0.72 V/rhe, which is found for Pt(100) during the positive going potential scan, could be related to the simultaneous presence of appreciable amounts of the two CO_{ad} adsorbates[63]. The lateral attractive interactions between CO_L and CO_B appear to be responsible for an additional blockage effect. The latter no longer exists during the negative going potential scan as the CO readsorption yields mainly CO_L species. Only at the lower switching potential the CO_B species can be newly formed. This interpretation accounts for the absence of this type of phenomenon for Pt(110) and Pt(111), as the corresponding current–potential profiles run in both potential directions appear in the same potential range, and are practically superimposed for Pt(111). At this stage it is necessary to emphasize the distinction between "electrocatalytic poisoning", which simply results from the presence of any type of CO_{ad}, and "surface blockage", which is only occasionally observed. The latter enhances the poisoning effect, through a mechanism involving the possible coupling of surface dipoles of opposite signs.

3.3. Surface roughness and poisoning effect

Recently it was found that the true surface area of pc noble metal electrodes such as Pt, Au, Rh, could be increased up to nearly 1000 times (at least for Pt) the initial geometric electrode area. The procedure to develop such increase in real electrode area is based upon the application of a periodic potential within certain potential limits at a frequency high enough to accumulate an hydrous metal oxide layer on the electrode surface, and subsequently to proceed to its electroreduction by means of a suitable potential programme[69].

The surface characteristics of this type of modified electrodes were firstly studied through scanning electron microscopy (SEM), later through scanning tunneling microscopy (STM)[69] and most recently by simultaneously combining the two techniques[70]. Accordingly, in the case of Pt, the surface topography compatible with the development of some roughness results from an ensemble of metal clusters and holes of about 10 nm average diameter[69]. For gold, the structure of the metal overlayer appears closer to a columnar- or brush-like structure, the diameter of each column, or of the channel left between them is also about 10 nm average diameter[69, 70]. This type of electrodes were denoted as "electrodispersed" or "cluster-like" type electrodes. A typical dome-like surface topography, as observed by STM for platinum and gold electrodes with a roughness factor of about 80, is shown in Figs 10a and b.

Generally speaking, the topography of electrodispersed noble metal electrodes, as depicted through STM, is heterogeneous. Thus, it is possible to distinguish the following different domains: (i) dominant
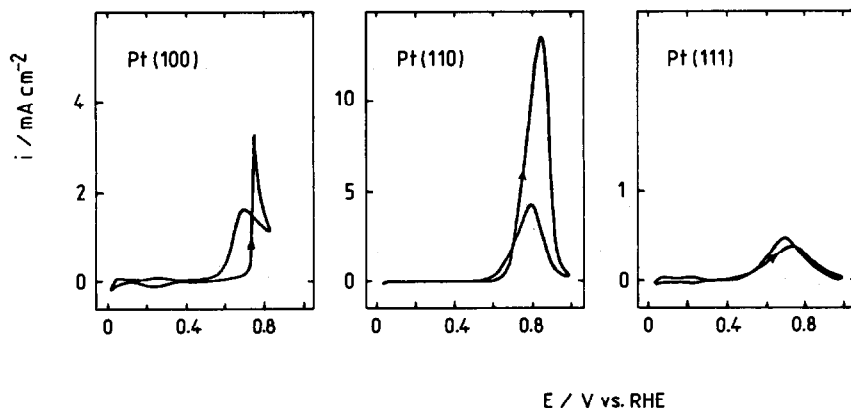
Fig. 9. Voltammograms of Pt(100), Pt(110) and Pt(111) single crystal electrodes in 0.5 M HClO$_4$+0.1 M CH$_3$OH solutions at 25°C and $v=50$ mV s^{-1}; only the first sweep is represented.
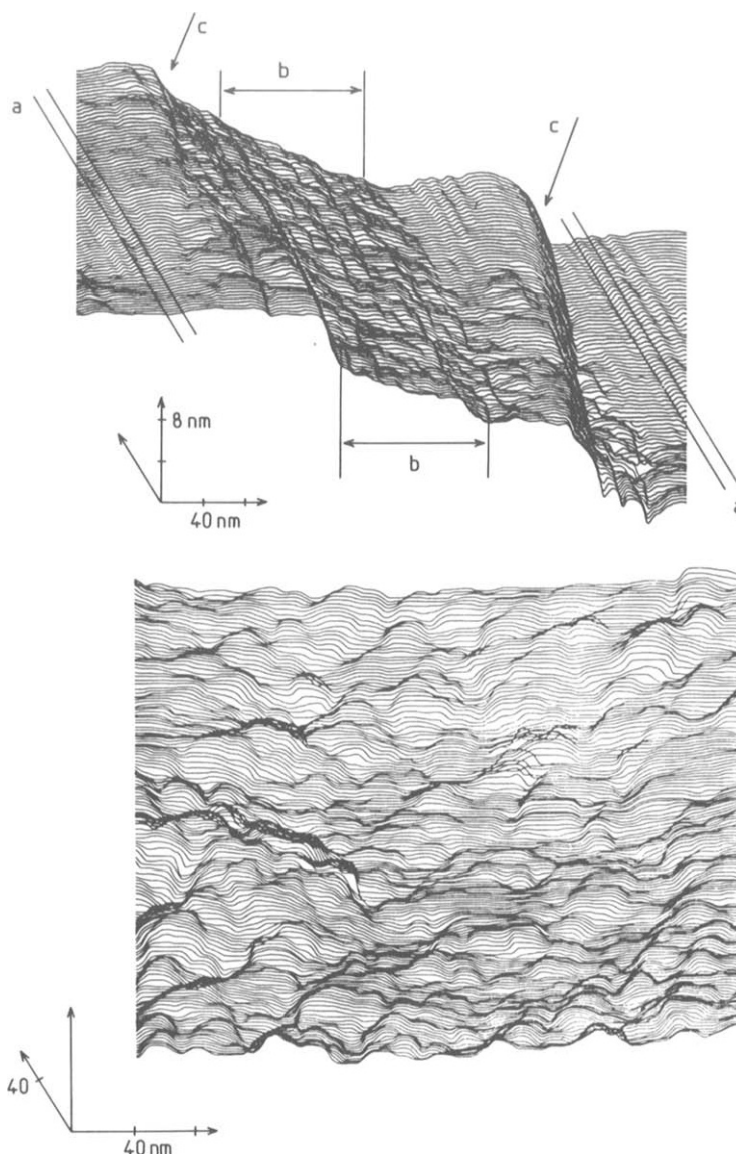
Fig. 10. (a) STM imaging of a Pt surface with a roughness factor of 80. Three different topographies can be distinguished (a, b, c). Regions of type b are responsible for high values of the roughness factor: (b) STM imaging of Au surface with a roughness factor of ≈ 80.

dome-like populated domains, which are directly responsible for the roughness and for the electrocatalytic properties of electrodispersed electrodes; (ii) small nearly flat domains with a well-defined corrugation, which are observed for reconstructed metal surfaces; (iii) domains with relatively large steps.

The uv–vis electroreflectance spectra of these electrode surfaces[71] show, particularly for platinum and gold, a new band at 1.8 eV in addition to that already known for the conventional metals. The new band comes from the characteristic topography of these surfaces. The dome-like protrusions favour the interactions between the surface plasmons and the components of the electric field of the incident electromagnetic radiation, as it is the case for large roughness silver surfaces[72].

The uv–vis electroreflection spectra of electrodispersed platinum and gold (rougness factor ≈ 14) are illustrated in Figs 11a and b. The corresponding spectra of the smooth surfaces have also been included for the sake of direct comparison.

From the electrochemistry standpoint it is important to investigate comparatively the adsorption and electrooxidation of CO and other small organic molecules on electrodispersed electrode surfaces. Electrodispersed platinum electrodes with roughness factors ranging from 5 to 250 have been tested for different electroactive species by using the microflux cell technique[73]. In presence of CO in solution, a complete surface coverage by CO_{ad} adsorbates can be achieved. As usually, the surface coverage is measured through the decrease in the H-adatom voltammetric
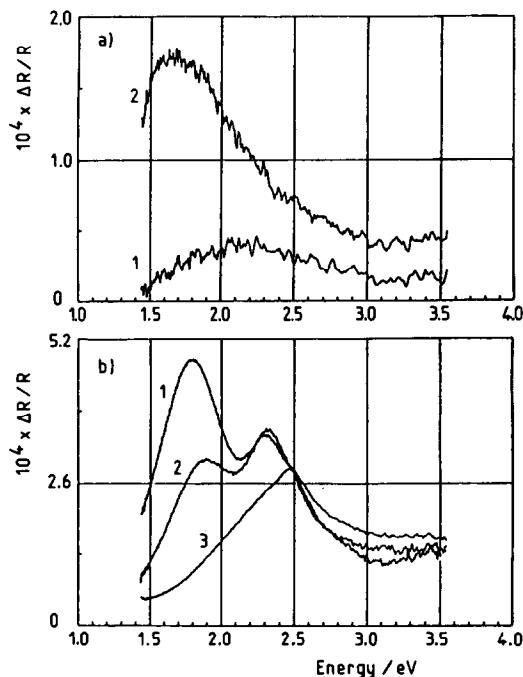
Fig. 11. (a) Electroreflectance spectra of smooth (1) and electrodispersed platinum (2); 0.3 M $HClO_4$; $\bar{E} = -0.25$ V vs mse; $\varphi = 40°$, p-polarization; $f = 22$ Hz; $\delta E = 30$ mV$_{(rms)}$; (b) Electroreflectance spectra of electrodispersed Au (1, 2) and pc smooth Au (3); 0.3 M $HClO_4$; $\bar{E} = 0.1$ V vs mse (1) and $\bar{E} = -0.3$ V vs mse (2, 3); $\varphi = 40°$; p-polarization; $f = 180$ Hz; $\delta E = 28$ mV$_{(rms)}$.

Fig. 12. EMIRS spectra of the adsorbed species resulting from the chemisorption of 1 M CH_3OH in 0.5 M $HClO_4$ at a rough Pt electrode. $f = 13.5$ Hz; 10 averaged scans. $\Delta E = 400$ mV; potential pulse centre (V vs rhe): (1) = 0.2; (2) = 0.3; (3) = 0.4; (4) = 0.5.

charge. However, a different situation arises for organic molecules, as in these cases the maximum surface coverage is only about 80–85% of the expected complete surface coverage. Furthermore, for roughness factors smaller than 30, the number and multiplicity of voltammetric peaks for CO electrooxidation depend strongly on the adsorption potential, E_{ad}. This dependence smooths down and practically disappears for higher roughness factors.

In terms of electrocatalytic activity, it appears that the electrodispersed electrodes exhibit a depolarizing effect, particularly noticeable for methanol and formic acid electrooxidation[73, 74].

The crystallite size of electrodispersed noble metal electrodes, as it should be expected from particle size effects in heterogeneous catalysis, plays a definite role on the chemisorption step. This also reflects in the fact that the rate of poisoning for electrodispersed electrodes is much lower than for smooth electrodes under comparable conditions[75].

The EMIRS experiment provides a deeper and clearer knowledge of the CO adsorbate formation throughout methanol chemisorption on electrodispersed platinum with a roughness factor equal to 20 (Fig. 12)[76]. The comparison has been made with smooth platinum. For a modulation potential of 400 mV amplitude and a mean potential value $\bar{E} = 0.2$ V/rhe, the electrodispersed platinum electrode shows only a relatively small amount of CO_L, a fact which correlates with a less important poisoning effect, as also noted by Kunimatsu et al.[77] for Pt electrodes roughened
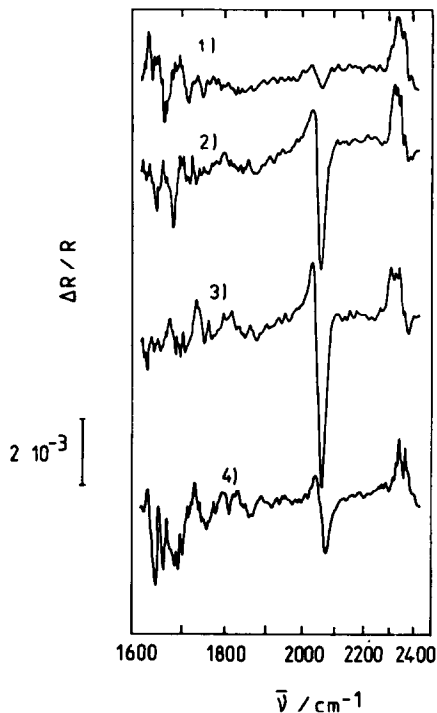
by potential cycling. Conversely, the CO_2 band becomes more intense and single-sided for any spectral accumulation time. Surely there is a clear difference in the behaviour of electrodispersed platinum as compared to that of smooth platinum (see Fig. 7) towards the chemisorption and electrooxidation of methanol[76]. On the other hand, when $\bar{E}$ is moved in the positive direction, one can observe that the intensity of the CO_L absorption band increases, but it remains very asymmetric because of a greater contribution at the positive potential limit. The intensity of this band goes through a maximum for $\bar{E} = 0.400$ V/rhe, a potential beyond which CO_{ad} is definitively oxidized to CO_2. The change of the spectrum with $\bar{E}$ suggests that a rather fast $CO_L \rightarrow CO_2$ conversion reaction becomes possible at the electrode[60]. Certainly, this question deserves further consideration as far as the formation of reduced CO_2 is concerned[74, 78, 79].

4. ADSORPTION OF CO ON ADATOM MODIFIED ELECTRODES, AS STUDIED BY EMIRS

After two decades of work it is now well-established that submonolayers of foreign metal adatoms underpotentially deposited on noble metals produce, in some cases, a considerable enhancement of the electrocatalytic activity of the substrates for the electrooxidation of several organic molecules[80, 81]. For in-

stance, in one of the most favourable cases, the under-potential electrodeposition of lead adatoms can increase the electrooxidation current of formic acid in acid medium, by a factor approximately equal to 60, when the oxidation is carried out on pc platinum electrodes, and by a smaller factor on pc rhodium electrodes[82].

On the other hand, EMIRS has clearly demonstrated the participation of CO_{ad} species during the chemisorption of both methanol and formic acid on platinum[23, 40, 83] and the role of CO as poison is now recognized (*Cf.* Section 3.1 and refs[5, 42, 84]).

The formation of a CO monolayer on rhodium results from the contribution of the three adsorbates, namely, CO_L, CO_B and CO_m (*cf.* Section 2.5). According to the quantitative analysis of the EMIRS bands, the distribution and surface concentration of each one of these species both depend on the nature of the molecule originally chemisorbed (CO, formic acid, methanol, . . .) and on the concentration of the electroactive species in solution[50, 54, 56, 85]. As an example, the relative composition of the "adsorbed" CO layer as a function of formic acid concentration in solution is given in Fig. 13. It is evident that a decrease in the concentration favours the formation of multi-bonded adsorbates.

4.1. *Perturbation of the CO_{ad} layer by adatoms*

The electrooxidation of formic acid has been recently investigated on rhodium covered with different surface concentrations of lead adatoms[54]. The latter was adjusted by properly setting the concentration of the precursor salt in solution (from 5×10^{-7} M to 10^{-3} M $Pb(ClO_4)_2$). The corresponding EMIRS spectra (Fig. 14) show that the CO_B species are specifically and gradually suppressed as the surface concentration of lead adatoms increases. The CO_B species disappears completely for 5×10^{-4} M $Pb (ClO_4)_2$, a value of salt concentration at which, according to Adžić and

Fig. 14. Series of EMIRS spectra of the adsorbed layer formed at a upd modified Rh electrode in 0.1 M HCOOH $+ 0.25$ M $HClO_4 + x$ M Pb^{2+} solutions (x was varied from 5×10^{-7} M to 1×10^{-3} M, as indicated in the figure). Spectral conditions: $\Delta E = 0.4$ V; $\bar{E} = 0.2$ V *vs rhe*, $f = 13.5$ Hz; 10 averaged scans.

Tripkovic[82], the maximum catalytic effect on the reaction is obtained. Simultaneously the relative distribution of other adsorbates, *i.e.* CO_L and CO_m, remains almost unchanged.

A very similar behaviour was also observed for the effect of copper adatoms on CO adsorption (from a CO-saturated solution) on rhodium (Fig. 15). These spectra were obtained by polarization modulation, and it was found that the CO_B species were almost completely removed by the upd of Cu adatoms, whereas the intensity of the CO_L *ir* band decreased only by *ca* 16%[26, 86].

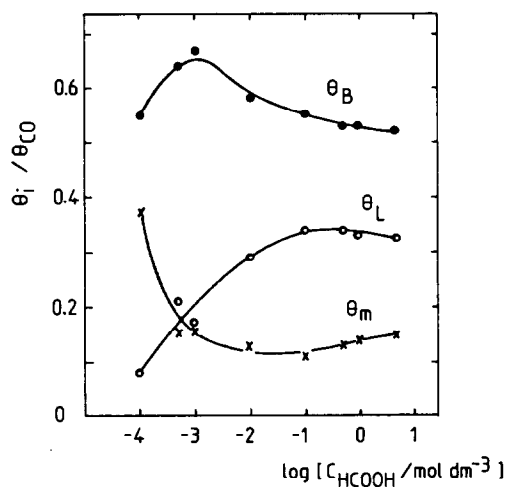As far as cadmium adatoms are concerned, their lack of activity towards the electrooxidation of formic

Fig. 13. Dependence of the relative coverage by each type of adsorbed CO species at a Rh electrode on the concentration of HCOOH in 0.25 M $HClO_4$: Θ_L, Θ_B and Θ_m correspond to linearly bonded CO, two-fold and multi-fold bridge-bonded CO, respectively.

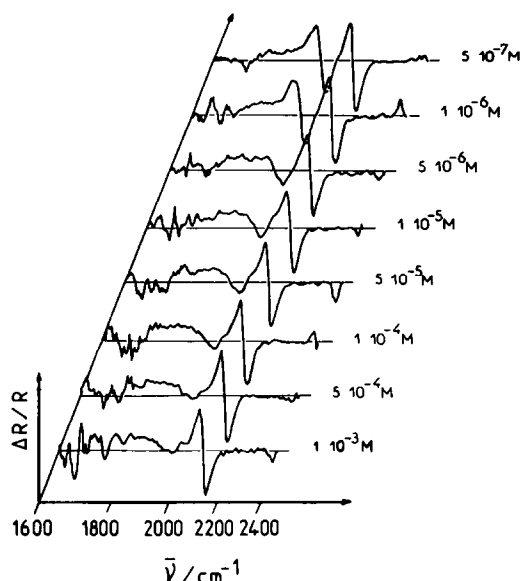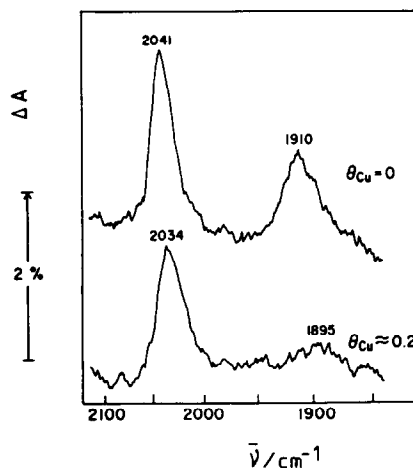Fig. 15. Effect of underpotentially deposited Cu adatoms on the PM-IRRAS spectra of CO adsorbed on pc Rh at 0.37 V *vs rhe.*

acid on rhodium could be found surprising. But for this case, EMIRS data show up a clear answer because the spectra corresponding to the CO_{ad} absorption region remain unchanged at the precursor salt concentration in solution usually employed. It appears that the adsorbability of cadmium is considerably lower than that of lead, in agreement with Adžič's original suggestion[82], so that cadmium adatoms are not able to displace, through competitive adsorption, the CO species from the surface. Can one extend this argument to the case of platinum? If one considers the two examples reported so far in the EMIRS literature, *ie* the influence of lead adatoms on the adsorption of formaldehyde in acid solutions[8, 87] and on the chemisorption of ethyleneglycol in basic solution[48], one can conclude seemingly that as the lead adatom concentration increases there is a selective disappearance of CO_{ad} species bound to more than one adsorption site before that the disappearance of CO_L can be observed. Thus, it is also possible that this type of mechanism on rhodium applies also to the case of platinum.

4.2. *General evaluation of the number of adsorption sites for adatoms and electrochemical correlation*

Let us consider again the electrooxidation of formic acid on rhodium modified electrodes to establish a correlation between the EMIRS and electrochemical data. With lead adatoms, the one-by-one replacement of a CO_B molecule by a Pb adatom, as observed by EMIRS (see Section 4.1), brings out to the conclusion that a lead adatom needs two adjacent adsorption sites, in accordance with the electrochemical results[88]. The EMIRS investigations have been extended to the study of the influence of bismuth adatoms. According to the electrochemical measurements each bismuth adatom requires three adsorption sites at the rhodium surface[88–90]. Hence, it is interesting to observe the perturbation induced by bismuth adatoms in the EMIRS bands of CO_{ad} species. Actually the CO_m species are not affected, whereas in the first instants of spectral accumulation, the CO_B band decreases and the CO_L band slightly increases. Such an unexpected behaviour can be explained provided that each bismuth adatom occupies three sites out of the four sites previously occupied by two adjacent CO_B adsorbates, the remaining site allowing the adsorption of CO_L species to occur[91]. Therefore, one has to admit that there is a good correlation between the spectroscopic data and the electrochemical measurements. It results that each lead adatom is bound to two sites, while each bismuth adatom is bonded to three sites at the surface. Similar experiments made with silver adatoms have shown a decrease in the CO_L EMIRS absorption band, still in agreement with electrochemical measurements according to which each silver atom is related to 1.15 site when adsorbed on rhodium[90].

5. THEORETICAL STUDY OF CO ADSORPTION ON MODEL SURFACES

Theoretical studies about CO adsorption on model solid metal substrates, particularly platinum, have

been made to explain adsorptive interactions in the gas phase–solid metal systems[92–98]. Similar studies can be extended to the liquid electrolyte–solid metal interface by considering the influence of the applied potential. Therefore for electrochemical systems, adsorption/desorption phenomena and the applied potential (electric perturbation) have to be considered as additional variables influencing the structure of the adsorbed layer.

5.1. *The* CO–Pt *adsorption bond*

The model, which gives a good description of the Pt–CO interaction, *ie* is the donation–retrodonation model, was originally proposed by Blyholder[99]. The valence orbitals contours of a CO molecule are illustrated in Figs 16a and b. The adsorption of CO results
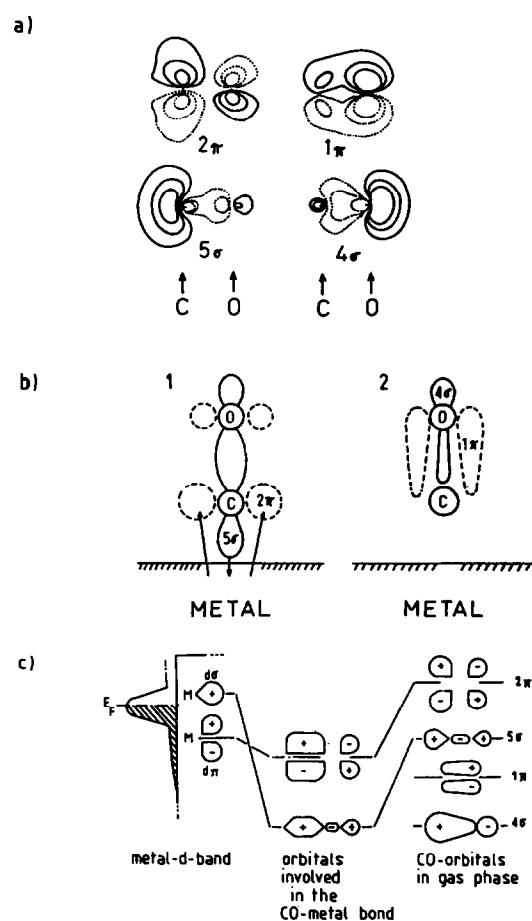
Fig. 16. (a) Valence orbitals contours of a CO molecule. Arrows indicate the location of C and O nuclei. 4σ, 5σ and π (or 1π) orbitals are occupied and π^* (or 2π) orbitals are unoccupied. (b) Adsorption scheme for CO on a metal surface according to the donation-retrodonation model. Full lines depict the 5σ orbital and dashed lines indicate the π^* orbitals: (1) orbitals which stabilize the adsorptive bond are depicted; (2) orbitals which play no significant role in the adsorptive bond are illustrated; (c) scheme for the CO-transition metal interaction. The CO-metal bond comprises the occupied bonding 5σ orbital and the empty π^* (2π) antibonding orbitals.

from two simultaneous bond stabilization effects, one produced throughout the electronic transfer from the 5σ-orbital of CO to the d-band (which displays a partial s-character) of platinum, and another one due to the retrodonation of electrons to the π^* (or 2π) antibonding orbitals of CO[99–101] (Fig. 16c).

5.2. Outline of the calculation procedure

The calculation of the CO–Pt interactions is made through the application of semiempirical methods, particularly those derived from the Extended Hükel Method (EHM) as originally developed by Hoffmann[102]. These methods allow the simulation of the applied potential through the corresponding shift of the band energy of the metal[103]. The metal phase is simulated as a metal cluster with a definite crystalline structure, for instance, Pt(111) and Pt(100). The size of the cluster results from a compromise between a negligible influence of the cluster borders on the CO–Pt bond interaction energy, and the computing facilities. Results recently reported are based upon two layered clusters, a Pt(111) cluster containing 19 atoms and a Pt(100) cluster of 25 atoms[103], with, for each cluster, a possible choice of different sites for CO–Pt interaction[104, 105]. The limitations regarding to the calculation procedures are inherent to the Quantum Chemistry methodology. The calculations proceed for the metal surface electrically discharged and for the metal surface charged with an excess of either positive (anodic applied potential) or negative charge (cathodic applied potential).

5.3. Uncharged Pt–CO adsorptive interaction

The calculations show that the adsorption of CO on platinum occurs without dissociation of the CO molecule, the C-atom being bound to the metal surface. The CO–Pt adsorptive bond appears with at least three types of configurations, namely, linear, bridge or hollow (multibonded) CO_{ad}[93–98]. The first configuration, CO_L, is the most favoured one on Pt(111), but both linear and bridge-forms exhibit the same adsorption energy on Pt(100)[100]. Therefore, these results imply a change in the adsorbate structure caused by the proper crystalline characteristics of the substrate.

For the Pt(111)–CO gas phase system involving a degree of surface coverage, Θ, equal to 1/3, an on-top linear coordination of CO produces a clear $(\sqrt{3} \times \sqrt{3})$ R30 LEED pattern, a structure which was originally assigned to adsorption at hollow sites. Likewise for $\Theta = 1/2$, the adsorbate involves one half linearly adsorbed (on-top) and one-half bridge adsorbed CO (hollow sites). The latter begins to appear at relatively low values of Θ. As Θ increases beyond 0.7, a compressed hexagonal structure with a $c(4 \times 2)$ unit cell in the (110) direction can be formed.

For Pt(100) a $c(2 \times 2)$ LEED structure is produced for $\Theta = 1/2$ with bridge bonded adsorbates. In this case linearly bonded CO appears for $\Theta \approx 0.66$ and the CO_L/CO_B ratio increases with the total coverage.

The Pt–CO interaction in aqueous solutions turns out to be more complex because of the simultaneous presence of water molecules at the interface. In this case water can play a double role, either as an

interacting dipole, or through its decomposition products, ie OH and H species. This fact opens the possibility to calculate the structure and stability of either CO_{ad} as the actual electrocatalytic poison or species such as Pt–COH, Pt–CHO, Pt–COOH, Pt–(CO_{ad}) (OH_{ad}), . . . which are presumably much closer to the real electrocatalytic intermediates in the electrooxidation of CO[106].

5.4. Charged Pt–CO adsorption interactions

When an external electric potential is applied to the Pt–CO (electrolyte solution) interface, the structural characteristics of CO-adsorbates change according to the applied potential, as expected. Negative applied potentials shift the CO adsorbate from one-fold to two-fold position and possibly to three-fold bonded on Pt(111)[107], due to the shift up in energy of the metal valence band lying closer to the energy of the empty π^* (or 2π) orbital level of CO[100, 101]. This fact strengthens the d–π^* orbital mixing, and favours CO adsorption at highly coordinated sites. Otherwise, positive applied potentials result in the stabilization of the one-fold coordination state[108]. It is the consequence of the metal d-band lowering that strengthens that 5σ-metal band interaction, the directional symmetry of the bond defining this coordination. The same trend was found for Pt(100), although in this case bridge and linear coordinations are equally favoured for the uncharged metal surface. Hence, for positive potential metal charging on both Pt(111) and Pt(100), adsorbed structures with linearly bonded CO appear to be the most favourable. At present, however, as only isolated adsorbed molecules have been theoretically considered[100, 101], no sound conclusions about changes in the structure of the adsorbed layer as a function of the potential applied to the metal can be derived. More sophisticated models have therefore to be worked out in the future.

Data obtained either by potential programme voltammetry (PPV) or by EMIRS, correlate well with the theoretical studies. It is clear, especially from PPV performed on Pt(hkl) electrodes that bridge and multibonded CO adsorbates are favoured at rather low adsorption potentials (near or in the hydrogen region), whereas for more positive potentials the linear coordination becomes predominant[7, 16, 17]. The same trend is also observed by EMIRS, although it is more difficult to conclude, due to the potential modulation. But it is roughly seen, especially for Pt(100) electrodes[62], that lowering the mean potential of the 400 mV potential pulse leads to a higher CO_B/CO_L ratio. This is also consistent with the results of Kunimatsu et al.[35, 37, 109] showing a higher concentration of CO_B when CO adsorbs on pc Pt in the hydrogen region, comparatively to its adsorption in the double layer region.

In conclusion, EHM calculations, complemented with mechanistic information recently reported, provide concrete data on the stability of the different adsorbates on the Pt(111) and Pt(100) cluster substrates, which are consistent with the experimental data reported so far. Thus, for the first time, it allows to advance a structural interpretation for the voltammetric behaviour of adsorbed CO electrooxidation on Pt single crystals[106]. For sufficiently positive appli-

ed potentials, the structure of the adsorbates is modified, and the changes can be related to those structures spectroscopically determined for the uncharged Pt–CO (gas phase) interface, but also to those for the charged Pt–CO (electrolytic solution) interface. Therefore, it appears that the multiplicity and location of the voltammetric peaks is not only the result of different CO coordination geometries on Pt, but it is also the result of cooperative interactions involving OH coadsorbed with different number of linearly adsorbed CO molecules.

6. CONCLUSIONS

The present review of information, concerning the adsorption and electrooxidation of CO, covers so many aspects that it justifies the selection of this process as a test reaction for electrocatalysis.

Accordingly, the following conclusions can be put forward.

(1) The electrooxidation of CO is a complex reaction, as it can be immediately deduced from the multiplicity of the voltammetric peaks that can be recorded in a relatively narrow potential range. Therefore, the study of such a process requires the use of several experimental techniques principally related to electrochemistry and surface spectroscopy.

(2) The structure and the distribution of the different CO species adsorbed on well defined surfaces, such as platinum single crystals, Pt(100) and Pt(111), as predicted by theoretical calculations (EHM), correlate well with the experimental results obtained both by cyclic voltammetry and EMIRS. Moreover the effect of the electrode potential on the CO adsorbates adlayer, as observed experimentally, is well predicted by the theoretical calculations, although the model is actually too simple to take into consideration lateral interactions between adsorbed CO and other adsorbates coming either from the electroactive species or from the solvent (water molecule).

(3) CO_{ad} is formed in the course of most electrochemical reactions involving the electrooxidation of small organic molecules. The kinetics of CO_{ad} formation depends upon different reaction parameters, such as the nature and the concentration of the electroactive species, the solution composition including pH, the adsorption time, the adsorption potential, the substrate surface characteristics, the electrooxidation potential program, etc. In any case, CO acts more as a catalytic poison than as a reactive intermediate[84].

(4) Both the formation of the CO_{ad} layer and the distribution of the three distinguishable types of adsorbates, which constitute the adsorbed layer, namely, CO_L, CO_B and CO_m, depend considerably on the kind of the electroactive species, ie its reactivity is related to its own structure and to the presence of reacting groups, and to the nature of the electrocatalytic metal.

The catalytic activity of the latter is closely related to the type of surface, ie smooth, polycrystal, single crystal, electrodispersed metal, preferred crystalline oriented metal.

The case of electrodispersed electrodes becomes particularly interesting. For these electrodes, which involve an enhancement of the roughness factor, and whose topography has been well-characterized throughout STM, the formation of CO_{ad} following the chemisorption of organic species, is appreciably diminished. The use of electrodispersed electrodes for practical systems (eg electrochemical generators, electrolyzers for organic synthesis, etc) is thus considered due to the mild poisoning effect of CO_{ad} species.

On the other hand, the electromodulated infrared spectroscopy came out as an in situ technique particularly useful to follow the change in the distribution of the different adsorbed species which constitute the adsorbed layer. EMIRS allows to obtain definite quantitative results concerning the selective suppression of the double bonded CO adsorbate caused by the presence of lead adatoms on the substrate. This "depoisoning" effect reflects in an increase of the electrooxidation current density, ie it turns out to be a true electrocatalytic effect. Furthermore, throughout EMIRS it is possible to study the perturbation of the CO_{ad} adsorbates and to evaluate from these data the number of adsorption sites needed for each metal adatom. From the systems which have already been investigated a good correlation between EMIRS and electrochemical data has been established.

REFERENCES

1. M. W. Breiter, Electrochemical Processes in Fuel Cells, (1969). Chs 6, 9 and 10, Springer Verlag, New York.
2. M. W. Breiter, in Modern Aspects of Electrochemistry (Edited by J. O'M. Bockris and B. E. Conway), vol. 10, Ch. 3, Plenum Press, New York (1975).
3. S. A. Bilmes, N. R. de Tacconi and A. J. Arvia, J. electrochem. Soc. 127, 2181 (1980); J. electroanal. Chem. 143, 179 (1983).
4. J. M. Léger, B. Beden and C. Lamy, Ber. Bunsenges. phys. Chem. 91, 336 (1987).
5. C. Lamy, Electrochim. Acta 29, 1581 (1984).
6. A. J. Arvia, Anal. Chem. 71, 944 (1975).
7. S. A. Bilmes, N. R. de Tacconi and A. J. Arvia, Proceedings of the Symposium on Electrocatalysis, the Electrochemical Society, Minneapolis, p. 276 (1981).
8. A. Bewick and B. S. Pons, in Infrared and Raman Spectroscopy (Edited by R. J. H. Clark and R. E. Hester), vol. 12, Ch. 1, Wiley Heyden, London (1985).
9. B. Beden and C. Lamy in Spectroelectrochemistry, Theory and Practice (Edited by R. J. Gale), Ch. 5, Plenum Press, New York (1988).

10. M. Cervino, W. E. Triaca and A. J. Arvia, *J. electroanal. Chem.* **182,** 51 (1985); *Electrochim. Acta,* **30,** 1323 (1985).
11. J. P. Randin, in *The Encyclopedia of the Electrochemistry of the Elements* (Edited by A. J. Bard), Vol. 7, Ch. 1, Marcel Dekker, New York (1976).
12a. B. B. Damaskin and V. E. Kazarinov, in *Comprehensive Treatise of Electrochemistry* (Edited by J. O'M. Bocksis *et al.*), vol. 1, p. 353, Plenum Press, New York (1984).
12b. J. Sobkowski and A. Czerwinski, *J. phys. Chem.* **89,** 365 (1985).
12c. M. Watanabe and S. Motoo, *J. electroanal. Chem.,* **206,** 197 (1986).
13. E. Santos and M. C. Giordano, Proceedings of the 34th ISE Meeting, Erlangen, Ext. Abstr. 0901 (1983).
14. S. A. Bilmes, N. R. de Tacconi and A. J. Arvia, *J. electroanal. Chem.* **164,** 129 (1984).
15. J. Clavilier, G. Guinet, R. Faure and R. Durand, *J. electroanal. Chem.* **107,** 205 (1980).
16. B. Beden, S. Bilmes, C. Lamy and J. M. Léger, *J. electroanal. Chem.* **149,** 295 (1983).
17. J. M. Léger, B. Beden, C. Lamy and S. Bilmes, *J. electroanal. Chem.* **170,** 305 (1984).
18. E. P. M. Leiva, E. Santos, M. C. Giordano, R. M. Cervino and A. J. Arvia, *J. electrochem. Soc.* **133,** 1660 (1986).
19. N. Collas, B. Beden, J. M. Léger and C. Lamy, *J. electroanal. Chem.* **186,** 287 (1985).
20. B. Beden, N. Collas, C. Lamy, J. M. Léger and V. Solis, *Surf. Sci.* **162,** 789 (1985).
21. A. Bewick, K. Kunimatsu and B. S. Pons, *Electrochim. Acta* **25,** 465 (1980).
22. A. Bewick, K. Kunimatsu, B. S. Pons and J. W. Russell, *J. electroanal. Chem.* **160,** 47 (1984).
23. B. Beden, A. Bewick, K. Kunimatsu and C. Lamy, *J. electroanal. Chem.* **142,** 345 (1982).
24. A. Bewick, *J. electroanal. Chem.* **150,** 481 (1983).
25. N. Sheppard and T. T. N'Guyen, in *Advances in Infrared and Raman Spectroscopy* (Edited by R. J. H. Clark and R. E. Hester), Vol. 5, Ch. 2, Wiley Heyden, London (1978).
26. R. O. Lezna, K. Kunimatsu and M. Enyo, *J. electroanal. Chem.* **258,** 115 (1989).
27. M. Choy de Martinez, B. Beden, F. Hahn and C. Lamy, *J. electron Spectrosc. Related Phenomena* **45,** 153 (1987).
28. T. Solomun, *Ber. Bunsenges. phys. Chem.* **90,** 556 (1986).
29. Y. Ikezawa, H. Saito, H. Matsubayashi and G. Toda, *J. electroanal. Chem.* **252,** 395 (1988).
30. A. Bewick, M. Razaq and J. W. Russell, *J. electroanal. Chem.* **256,** 165 (1988).
31. K. Kunimatsu and A. Bewick, *Ind. J. Technol.* **24,** 407 (1986).
32. J. W. Russell, J. Overend, K. Scanlon, M. W. Severson and A. Bewick, *J. phys. Chem.* **86,** 205 (1982).
33. S. Pons, T. Davidson and A. Bewick, *J. electroanal. Chem.* **160,** 63 (1984); S. Pons, *J. electroanal. Chem.* **160,** 369 (1984).
34. M. A. Habib and J. O'M. Bockris, *J. electroanal. Chem.* **180,** 207 (1984).
35. W. G. Golden, K. Kunimatsu and H. Seki, *J. phys. Chem.* **88,** 1275 (1984); K. Kunimatsu, H. Seki, W. G. Golden, J. G. Gordon II and M. R. Philpott, *Surf. Sci.* **158,** 596 (1985).
36. K. Kunimatsu and H. Kita, *J. electroanal. Chem.* **218,** 155 (1987).
37. K. Kunimatsu, W. G. Golden, H. Seki and M. R. Philpott, *Langmuir* **1,** 245 (1985).
38. D. K. Lambert, *J. electron Spectrosc. Related Phenomena* **30,** 59 (1983); *Solid St. Commun.* **51,** 297 (1984).
39. P. P. Schmidt, M. W. Severson, C. Korzeniewski and S. Pons, *J. electroanal. Chem.* **225,** 267 (1987); M. R. Anderson, D. Blackwood and S. Pons, *J. electroanal. Chem.* **256,** 387 (1988); M. R. Anderson, D. Blackwood,

40. T. G. Richmond and S. Pons, *J. electroanal. Chem.* **256,** 397 (1988).
40. B. Beden, C. Lamy, A. Bewick and K. Kunimatsu, *J. electroanal. Chem.* **121,** 343 (1981); A. Bewick, K. Kunimatsu, B. Beden and C. Lamy, Proceedings of the 32nd ISE Meeting Dubrovink/Cavtat, Yugoslavia, Ext. Abstr. A28, p. 92 (1981).
41. B. Beden, A. Bewick and C. Lamy, *J. electroanal. Chem.* **148,** 147 (1983).
42. B. Beden, in *Spectroscopic and Diffraction Techniques in Interfacial Electrochemistry* (Edited by C. Gutierrez), Reidel, Holland, in press.
43. V. S. Bagotsky, Yu. B. Vassiliev and O. A. Khazova, *J. electroanal. Chem.* **81,** 229 (1977).
44. E. Sokolova, *Electrochim. Acta* **20,** 323 (1975).
45. K. Kunimatsu, *J. electroanal. Chem.* **213,** 149 (1986).
46. O. Wolter and J. Heitbaum, *Ber. Bunsenges. phys. Chem.* **88,** 2 (1984); O. Wolter, J. Willsau and J. Heitbaum, *electrochem. Soc.* **132,** 1635 (1985); *J. Willsau* and *J. Heitbaum, J. electroanal. Chem.* **185,** 181 (1985); *Electrochim. Acta.* **31,** 943 (1986).
47. H. W. Buschmann, S. Wilhelm and W. Vielstich, *Electrochim. Acta.* **31,** 939 (1986); T. Iwasita, W. Vielstich and E. Santos, *J. electroanal. Chem.* **229,** 367 (1987).
48. F. Hahn, B. Beden, F. Kadirgan and C. Lamy, *J. electroanal. Chem.* **216,** 169 (1987).
49. P. A. Christensen and A. Hamnett, *J. electroanal. Chem.* **260,** 347 (1989).
50. B. Beden, M. C. Morin, F. Hahn and C. Lamy, *J. electroanal. Chem.* **229,** 353 (1987); J. M. Perez, B. Beden, F. Hahn, A. Aldaz and C. Lamy, *J. electroanal. Chem.* **262,** 251 (1989).
51. L. W. H. Leung and M. J. Weaver, *J. electroanal. Chem.* **240,** 341 (1988); *J. phys. Chem.* **92,** 4019 (1988).
52. T. Iwasita and W. Vielstich, *J. electroanal. Chem.* **257,** 319 (1988).
53. T. Solomun, *Surf. Sci.* **176,** 593. (1986).
54. M. Choy de Martinez, B. Beden, F. Hahn and C. Lamy, *J. electroanal. Chem.* **249,** 265 (1988).
55. P. A. Christensen, A. Hamnett and S. A. Weeks, *J. electroanal. Chem.* **250,** 127 (1988).
56. B. Beden, F. Hahn, S. Juanto, C. Lamy and J. M. Léger, *J. electroanal. Chem.* **225,** 215 (1987).
57. R. J. Nichols and A. Bewick, *Electrochim. Acta* **33,** 1691 (1988).
58. J. O'M. Bockris and B. Yang, *J. electrochem. Soc.* **252,** 209 (1988).
59. B. Beden, F. Hahn, J. M. Léger, C. Lamy and M. I. Lopes, *J. electroanal. Chem.* **258,** 463 (1989).
60. J. M. Perez, F. Hahn, B. Beden and C. Lamy, Proceedings of the 4th Meeting of the Portuguese Electrochemical Society, Lisbon (1989).
61. D. S. Corrigan, E. K. Krauskopf, L. M. Rice, A. Wieckowski and M. J. Weaver, *J. phys. Chem.* **92,** 1596 (1988).
62. S. Juanto, B. Beden, F. Hahn, J. M. Léger and C. Lamy, *J. electroanal. Chem.* **237,** 119 (1987).
63. B. Beden, S. Juanto, F. Hahn, J. M. Léger and C. Lamy, *J. electroanal. Chem.* **238,** 323 (1987).
64. S. G. Sun, J. Clavilier and A. Bewick, *J. electroanal. Chem.* **240,** 147 (1988).
65. F. Kitamura, M. Taiseda, M. Takahashi and M. Ito, *Chem. Phys. Lett.* **142,** 318 (1987).
66. N. Furuya, S. Motoo and K. Kunimatsu, *J. electroanal. Chem.* **239,** 347 (1988).
67. M. Tüshaus, E. Schweizer, P. Hollins and A. M. Bradshaw, *J. electron Spectrosc. Related Phenomena* **44,** 305 (1987).
68. L. W. H. Leung, A. Wieckowski and M. J. Weaver, *J. Phys. Chem.,* **192,** 6985 (1988). *J. electroanal. Chem.,* 93 (1983); **171,** 393 (1984).
69. A. C. Chialvo, W. E. Triaca and A. J. Arvia, *J. electroa-*

nal. Chem. **146,** 93 (1983); **171,** 393 (1984); L. Vasquez, J. Gomez, A. M. Baro, A. Garcia, M. L. Marcos, J. Gonzalez-Velasco, J. M. Vara, A. J. Arvia, J. Presa, A. Garcia and M. Aguilar, *J. Am. chem. Soc.* **109,** 1730 (1987).

70. L. Vasquez, A. Bartolome, A. M. Baro, C. Alonso, R. C. Salvarezza and A. J. Arvia, *Surf. Sci.* in press.
71. R. O. Lezna, N. R. de Tacconi, C. L. Perdriel and A. J. Arvia, Proceedings of the 171ˢᵗ Meeting of the Electrochemical Society, Philadelphia (Edited by S. Srinivasan), p. 31 (1988).
72. M. Abraham and A. Tadjeddine, *Surf. Sci.* **173,** 65 (1986).
73. A. M. Castro Luna, M. C. Giordano and A. J. Arvia, *J. electroanal. Chem.,* **259,** 173 (1989).
74. M. L. Marcos, J. M. Vara, J. Gonzalez-Velasco and A. J. Arvia, *J. electroanal. Chem.* **224,** 189 (1987).
75. A. M. Castro Luna, A. E. Bolzan, M. F. L. de Mele and A. J. Arvia, *Z. phys. Chem.,* in press.
76. B. Beden, F. Hahn, C. Lamy, J. M. Leger, N. R. de Tacconi, R. O. Lezna and A. J. Arvia, *J. electroanal. Chem.* **261,** 401 (1989).
77. K. Kunimatsu, K. Shimazu and H. Kita, *J. electroanal. Chem.* **256,** 371 (1988).
78. J. Giner, *Electrochim. Acta* **8,** 857 (1963); **9,** 63 (1964).
79. B. Beden, A. Bewick, M. Razaq and J. Weber, *J. electroanal. Chem.* **139,** 203 (1982).
80. R. R. Adžić, *Israel J. Chem.* **18,** 160 (1979).
81. R. R. Adžić, in *Advances in Electrochemistry and Electrochemical Engineering* (Edited by H. Gerischer and C. W. Tobias), Vol. 13, p. 159, Wiley-Interscience, New York (1984).
82. R. R. Adzić and A. V. Tripkovic, *J. electroanal. Chem.* **99,** 43 (1979).
83. B. Beden, A. Bewick, K. Kunimatsu and C. Lamy, *J. electroanal. Chem.* **150,** 505 (1983).
84. R. Parsons and T. Vandernoot, *J. electroanal. Chem.* **257,** 9 (1988).
85. M. Choy de Martinez, Thèse de l'Université de Poitiers (1988).
86. R. O. Lezna, K. Kunimatsu and M. Enyo, V Simposio Brasileno de Electroquimica e Electroanalitica, Sâo Paolo (1986).
87. A. Bewick, in *Trends in Interfacial Electrochemistry* (Edited by A. F. Silva), NATO ASI Series, Reidel, Dordrecht Vol. 179, p. 331, (1986).

88. M. Watanabe and S. Motoo, *J. electroanal. Chem.* **202,** 137 (1986); S. Motoo and M. Watanabe, International Conference on the Structure and Dynamics of the Solid/Electrolyte Interface, Berlin (1986).
89. B. Parajon Costa, Ph.D. Thesis, INIFTA, La Plata 1986.
90. N. Furuya and S. Motoo, *J. electroanal. Chem.* **107,** 159 (1980).
91. B. Beden, M. Choy de Martinez and C. Lamy, VIII Réunion Latino America de Electroquimica y Corrosion, Cordoba (1988).
92. G. Ertl, M. Neumann and K. M. Streit, *Surf. Sci.* **64,** 393 (1977).
93. L. K. Verheij, J. Lux, A. B. Anton, B. Belsenna and G. Comsa, *Surf. Sci.* **182,** 390 (1987).
94. A. M. Lahee, J. P. Toennies and C. Wöhl, *Surf. Sci.* **177,** 371 (1986).
95. H. Steininger, S. Lehwald and I. Ibach, *Surf. Sci.* **123,** 264 (1982).
96. Shin-Ishi, Y. Ohno and B. Viswanathan, *Surf. Sci.,* **161,** 349 (1985).
97. J. P. Biberian and M. A. Van Hove, *Surf. Sci.* **118,** 443 (1982).
98. J. P. Biberian and M. A. Van Hove, *Surf. Sci.,* **138,** 361, (1984).
99. G. Blyholder, *J. phys. Chem.* **68,** 2772 (1964).
100. A. B. Anderson and M. K. Awad, *J. Am. chem. Soc.* **107,** 7854 (1985).
101. N. K. Ray and A. B. Anderson, *Surf. Sci.* **125,** 803 (1983).
102. R. Hoffmann, *J. chem. Phys.* **39,** 1397 (1963).
103. G. Estiü, S. A. Maluendes, E. A. Castro and A. J. Arvia, *J. phys. Chem.* **92,** 2512 (1988).
104. R. P. Messner, in *The Nature of the Surface Chemical Bonding* (Edited by T. N. Rhodin and G. Ertl), Ch. II, North Holland, Amsterdam (1979).
105. G. Ertl, in *The Nature of the Surface Chemical Bonding* (Edited by T. N. Rhodin and G. Ertl), Ch. V, North Holland, Amsterdam (1979).
106. G. Estiü, S. A. Maluendes, E. A. Castro and A. J. Arvia, *J. phys. Chem.* Submitted.
107. E. L. Garfunkel, J. E. Crowell and G. A. Somorjai, *J. phys. Chem.* **86,** 310 (1982).
108. N. K. Ray and A. B. Anderson, *J. phys. Chem.* **86,** 4851 (1982).
109. K. Kunimatsu, H. Seki, W. G. Golden, J. G. Gordon II and M. R. Philpott, *Langmuir* **2,** 464 (1986).